Solid State Communications 251 (2017) 79–87

Contents lists available at ScienceDirect

Solid State Communications

journal homepage: www.elsevier.com/locate/ssc

Communication

Magnetism and thermodynamics of the anisotropic frustrated spin-1 Heisenberg antiferromagnet on a body-centered cubic lattice

Bin-Zhou Mi[a,b,*]

[a] Department of Physics, School of Mathematics and Physics, University of Science and Technology Beijing, Beijing 100083, China
[b] Department of Basic Curriculum, North China Institute of Science and Technology, Beijing 101601, China

ARTICLE INFO

Keywords:
A. Frustrated spin-1 Heisenberg antiferromagnet
D. Thermodynamic properties
C. Spin anisotropy and single-ion anisotropy
E. Double-time Green's function method

ABSTRACT

The magnetic and thermodynamic properties of anisotropic frustrated spin-1 Heisenberg antiferromagnet on a body-centered cubic lattice for Néel phase (the region of weak frustration) are systematically investigated by use of the double-time Green's function method within the random phase approximation and the Anderson and Callen's decoupling. The zero-temperature sublattice magnetization and Néel temperature increase with spin anisotropy strength and single-ion anisotropy strength, and decrease with frustration strength. This indicates that quantum fluctuation is suppressed by spin anisotropy and single-ion anisotropy, by contrast, is strengthened by frustration. It is possible to tune the quantum fluctuations by the competition of anisotropy strength and frustration strength to change the ground state properties of magnetic materials. Although we find that both the spin anisotropy and the single-ion anisotropy suppress the quantum fluctuations, but their respective effects on the thermodynamic quantities, especially the internal energy and free energy, are different at zero temperature and finite temperature. Furthermore, when these two kinds of anisotropic coexist, the effect of the spin anisotropy on the sublattice magnetization and internal energy is larger than that of the single-ion anisotropy.

1. Introduction

Frustrated quantum antiferromagnets with competing nearest neighbor (nn) and next nearest neighbor (nnn) antiferromagnetic exchange interactions, J_1 and J_2 respectively, have been at the center of intense experimental and theoretical investigations in condensed matter physics for more than two decades [1–3]. A well-known example is the spin-1/2 J_1-J_2 quantum Heisenberg model on a two dimensional (2D) square lattice. This model could be used to describe the magnetic structures in real materials. For small J_2 values, this model has been used to describe antiferromagnetic properties of the copper oxide monolayers in the Cu-based high-temperature oxide superconductors [4,5]. For large J_2, the antiferromagnetic materials Li_2VOSiO_4 and Li_2VOGeO_4 can also be described by this model [6,7]. Furthermore, the most representative structure that could be well described by this model might be the Fe-As monolayers in the Fe-base superconductors LaOFeAs [8–14] and $BaFe_2As_2$[15]. Because of its importance, spin-1/2 J_1-J_2 quantum Heisenberg model on the square lattice has been studied extensively by various theoretical techniques and numerical methods [16–29]. At low temperature 2D square lattice Heisenberg antiferromagnets exhibit new types of magnetic order and novel quantum phases. Without nnn exchange interaction (J_2=0), the ground state is known to be ordinary antiferromagnet. A nonzero nnn exchange interaction induces the frustration and breaks the antiferromagnetic ordering. The competition between the nn and nnn exchange interactions is characterized by the frustration strength J_2/J_1. The zero-temperature phase diagram displays strong dependence on the frustration strength. It has been found that [28] the two magnetically ordered phases, Néel order for $J_2/J_1 \leq 0.4$, and collinear order for $J_2/J_1 \geq 0.6$, are separated by a nonmagnetic disordered region at $0.4 \leq J_2/J_1 \leq 0.6$, where a gapped quantum spin liquid phase is found. The quantum phase transition at J_2/J_1=0.4 is of the second order while the one at J_2/J_1=0.6 is of the first order and the spin gaps cross linearly at J_2/J_1=0.5. The properties of the quantum spin liquid are a current field of active research, and the precise nature of the nonmagnetic disordered state is still under debate. We here present a few words more to discuss the quantum spin liquids. It is generally believed that low dimensionality is essential for the formation of a quantum spin liquid due to fluctuation effects in lattice systems strengthen with decreasing coordination number. So the majority of research works in the field

* Correspondence address: Department of Physics, School of Mathematics and Physics, University of Science and Technology Beijing, Beijing 100083, China. Tel.: +86 1062316177; +86 13582467082.
E-mail address: mbzfjerry2008@126.com.

http://dx.doi.org/10.1016/j.ssc.2016.12.009
Received 6 October 2016; Received in revised form 5 December 2016; Accepted 15 December 2016
Available online 16 December 2016

have focused on the 2D systems, while three-dimensional (3D) quantum spin liquids are very scarce because they are harder to stabilize. However, some notable exceptions are frustrated 3D systems like the Heisenberg antiferromagnet on the body-centered tetragonal (BCT) lattice [30] and pyrochlore lattice [31,32], where the rich stable spin-liquid phases are observed. The geometrically frustrated BCT lattice, in particular, is realized in several strongly correlated electron materials, and studied for many years [33–42], following the pioneering study by Villian [33]. In recent years, the magnetism and phase transition of the anisotropic frustrated Heisenberg antiferromagnet model on a 2D square lattice are studied in Refs. [29,43–52]. For the case of anisotropy, the focus of the study is to discuss the effect of anisotropy on the zero-temperature phase diagram and possible phase transition at finite temperature. Compared with the quantum phase transition, very few studies have been carried out on the finite-temperature phase transition [50–52].

The magnetic properties of frustrated spin models strongly depend on the dimensionality (d), Hamiltonian symmetry (n) and spin quantum number (S). Compared with the 2D case, the 3D J_1-J_2 Heisenberg antiferromagnet model on the body-centered cubic (bcc) lattice that has been studied [53–58] in detail up to now are quite rare, especially its thermodynamics at finite temperature [59,60], and the ground-state property seems to be not so clear yet. Contrary to the 2D quantum spin-1/2 Heisenberg J_1-J_2 model (n=3) on the square lattice, these studies [54–57] show that the 3D quantum spin-1/2 Heisenberg J_1-J_2 model (n=3) on the bcc lattice does not have a disordered spin liquid phase and have a direct first-order quantum phase transition from the Néel phase to collinear phase occurs at critical value $(J_2/J_1)_c \approx 0.70$. However, Fig. 4 in the Ref. [58] shows that increasing J_2 reduces the sublattice magnetization in the Néel phase, eventually destroying the long range order at $J_2/J_1 \approx 0.65$. It is also shows that the collinear phase emerges at $J_2/J_1 \approx 0.7$. It is implied that there might be an unknown region at $0.65 \le J_2/J_1 \le 0.7$. In other words, double-time Green's function method within random phase approximation (RPA) alone in the Ref. [58] cannot resolve whether or not a transition from the Néel phase to the quantum spin-liquid phase occurs or the Néel phase directly transitions to the collinear phase. Importantly, as mentioned above, spin-liquid state can be stabilized in a 3D Heisenberg frustration J_1-J_2-J_3 model on the BCT lattice, which has similar lattice structure with bcc. The method introduced in Ref. [30] can be generalized to the bcc lattice. Most interestingly, the recent study [30] by Carlene Farias et al. opens a window for the realization of unconventional quantum ground-state in 3D materials. Therefore, the concerned unknown region at $0.65 \le J_2/J_1 \le 0.7$ for bcc lattice should be further studied using effective theoretical techniques in the future. For the bcc lattice, the Néel phase can be described by a standard two sublattice system as in the case of 2D models, while the collinear phase can be properly described with four sublattices. For the classical Heisenberg J_1-J_2 model and the Ising J_1-J_2 model on the bcc lattice, the mean field calculation [53] gives $(J_2/J_1)_{MF}=2/3$ for its critical transition point. Recently it is worth noting that the magnetic properties of iron-based high-temperature superconductors need to be described by a frustrated 3D Heisenberg spin J_1-J_2-$J_c$model [61–64], and the spin quantum number greater than 1/2 [65–67]. The bcc structure is one standard 3D lattice type that can be realized in several systems [68–70]. In addition, anisotropies, either spin anisotropy or single-ion anisotropy, are quite common in real materials, and which originate from very different physical mechanisms. It is expected that these two kinds of anisotropy strongly suppress the quantum fluctuations. Studying the effect of anisotropy can help us understand the role of quantum and thermodynamic fluctuations in phase transitions [29]. Seen from the perspective of the theory, a suitable model that takes into account such asymmetries is the so-called anisotropic frustrated Heisenberg J_1-J_2 model in the presence of the spin and single-ion anisotropies. Therefore, the 3D anisotropic frustrated system thermodynamics for spin-1 is important, but up to present rather poorly investigated.

Motivated by the above considerations, in this paper, we investigate thermodynamic properties of the quantum J_1-J_2 spin-1 Heisenberg antiferromagnet with spin and single-ion anisotropies on a bcc lattice and focus on the region of weak frustration $J_2/J_1 < (J_2/J_1)_{MF}=2/3$, i.e., Néel phase. The rest of this paper is organized as follows. In Section 2 we put down the Hamiltonian of 3D anisotropic frustrated spin-1 Heisenberg J_1-J_2 model on the bcc lattice for Néel phase. Then we briefly outline the formulas derived by the double-time Green's function method. In Section 3, numerical computation is carried out and discussed. At last, Section 4 presents our concluding remarks.

2. Model and formulas

The Hamiltonian of the frustrated anisotropic spin-1 Heisenberg antiferromagnet on a bcc lattice for Néel phase considered in this paper is given by

$$\begin{aligned} H = {} & J_1 \sum_{\langle 1i,2j\rangle} [(1-\Delta)(S_{1i}^x S_{2j}^x + S_{1i}^y S_{2j}^y) + S_{1i}^z S_{2j}^z] \\ & + \frac{J_2}{2} \sum_{<1i,1i'>} [(1-\Delta)(S_{1i}^x S_{1i'}^x + S_{1i}^y S_{1i'}^y) + S_{1i}^z S_{1i'}^z] \\ & + \frac{J_2}{2} \sum_{<2j,2j'>} [(1-\Delta)(S_{2j}^x S_{2j'}^x + S_{2j}^y S_{2j'}^y) + S_{2j}^z S_{2j'}^z] - D \sum_{1i} (S_{1i}^z)^2 \\ & - D \sum_{2j} (S_{2j}^z)^2, \end{aligned} \tag{1}$$

Here $1i$ and $2j$ denote the site on the sublattice 1 and 2, respectively. The [1i,2j] means that the nn exchanges are involved, and the $(1i,1i')$ and $(2j,2j')$ indicate that the nnn exchanges are included. Where $S_{\alpha i}^x$, $S_{\alpha i}^y$, and $S_{\alpha i}^z$ (α=1, or 2) represent the three components of the spin-1 operator for a spin at site αi. Both the nn and nnn exchanges J_1 and J_2 are assumed to be positive, so that it was believed to be a frustrated antiferromagnetic system. The first term represents the Heisenberg nn exchanges between two sublattice. The second term and third term describe the Heisenberg nnn exchanges of each sublattice 1 and 2, respectively. Δ denotes the spin anisotropic strength with $0 \le \Delta \le 1$ for the nn and nnn interactions. The fourth and fifth term describe the single-ion anisotropy of sublattice 1 and 2, respectively. D represents the single-ion anisotropy strength for two sublattice. When D=0, the above Hamiltonian stands for the isotropic Heisenberg J_1-J_2 model for Δ=0, and the Ising J_1-J_2 model for Δ=1. Spin anisotropy and single-ion anisotropy may exist in many real magnetic materials. More importantly, we can adjust the quantum and thermodynamic fluctuations by introducing anisotropy. Therefore, the study of the Hamiltonian Eq. (1) is meaningful. For the bcc lattice the number of nn and nnn are z_1=8 and z_2=6. In this paper, for the sake of convenience, we set Boltzman constant k_B=1. In calculation, we fix J_1=1, and focus on the parameter regime $0 \le J_2 < 2/3$, where the Néel antiferromagnetic ground-state is realized. Hereafter, denoted as J_2/J_1, and called as frustration strength, and all parameters, including spin anisotropic strength Δ, single-ion anisotropy strength D, temperature T, and sublattice magnetization $\langle S^z \rangle$ are taken as dimensionless quantities.

The double-time Green's function method is a powerful tools [71–76] to deal with Heisenberg magnetic systems [77–80] since this method takes into account the quantum fluctuation, and is valid in the whole temperature range. Moreover, the double-time Green's function method gives good agreement with quantum Monte Carlo (QMC) simulations in a wide temperature range of the ordered phase [75]. In order to study magnetic and thermodynamic properties of 3D anisotropic spin-1 J_1-J_2 model on bcc lattice, we follow our previous investigation of this model in the isotropic case [60] and introduce the retarded Green's function

$$G(t-t') = \langle\langle \mathbf{A}^T; \mathbf{B} \rangle\rangle = -i\theta(t-t')\langle \mathbf{A}^T\mathbf{B} - \mathbf{B}\mathbf{A}^T \rangle, \tag{2}$$

where the operators $\boldsymbol{A}$ and $\boldsymbol{B}$ are actually operator vectors in the following form:

$$\mathbf{A} = (S_1^+, S_2^+),$$
$$\mathbf{B} = (\exp(uS_1^z)S_1^-, \exp(uS_2^z)S_2^-), \tag{3}$$

and u is the Callen parameter [71]. In Eq. (2), the Green's function is in fact an 2×2 matrix, and its Fourier component is denoted as $\mathbf{g}(\omega)$. Then the equation of motion of the Green's function $\mathbf{g}(\omega)$ will be obtained by standard procedure [75,76]. The higher order Green's functions need to be decoupled. For the terms concerning Heisenberg exchange interaction in Eq. (1), we use the RPA decoupling [75,76]. For the terms concerning single-ion anisotropy in Eq. (1), we adopt the Anderson and Callen's (ACs) decoupling [75,76]. The derivation is lengthy but straight forward following the standard routine, and here we do not intend to give its details. In the following, the calculation formulas of thermodynamic quantities are presented. They are the sublattice magnetization $\langle S_\mu^z\rangle$, Néel temperature T_N, internal energy $E(T)$, and free energy $F(T)$. The sublattice magnetization is expressed [71,75,76] as follows,

$$\langle S_\mu^z\rangle = \frac{(\Phi_\mu + 1 + S)\Phi_\mu^{2S+1} - (\Phi_\mu - S)(\Phi_\mu + 1)^{2S+1}}{(\Phi_\mu + 1)^{2S+1} - \Phi_\mu^{2S+1}}, (\mu = 1, 2), \tag{4}$$

where

$$\Phi_\mu = \frac{2}{N}\sum_{\mathbf{k}}\sum_{\tau=1}^{2}\frac{U_{\mu\tau}U_{\tau\mu}^{-1}}{e^{\beta\omega_\tau} - 1}. \tag{5}$$

where $\beta = 1/T$, the inverse of temperature. Since the lattice is divided into two sublattices, there are two branches of spin wave dispersion relationships:

$$\omega_\mu = \sqrt{[J_{10} - J_{20} + (1 - \Delta)J_2(\mathbf{k}) + 2DC_\mu]^2 - [(1 - \Delta)J_1(\mathbf{k})]^2}\,\langle S_\mu^z\rangle,$$
$$(\mu = 1, 2). \tag{6}$$

In Eq. (6), $J_{10} = z_1J_1$, $J_{20} = z_2J_2$,

$$J_1(\mathbf{k}) = J_{10}\cos\left(\frac{1}{2}k_xa\right)\cos\left(\frac{1}{2}k_ya\right)\cos\left(\frac{1}{2}k_za\right), \tag{7}$$

$$J_2(\mathbf{k}) = \frac{1}{3}J_{20}[\cos k_xa + \cos k_ya + \cos k_za], \tag{8}$$

$$C_\mu = 1 - \frac{1}{2S^2}[S(S + 1) - \langle S_\mu^zS_\mu^z\rangle], (\mu = 1, 2), \tag{9}$$

and

$$\langle S_\mu^zS_\mu^z\rangle = S(S + 1) - (1 + 2\Phi_\mu)\langle S_\mu^z\rangle. \tag{10}$$

where the wave vectors along the x, y, and z directions are denoted by k_x, k_y, and k_z. The distance between the nn sites is a. The matrix $\boldsymbol{U}$ and its inverse$\boldsymbol{U}^{-1}$ in Eq. (5)are as follows,

$$\mathbf{U} = \begin{pmatrix} 1 & 1 \\ \frac{[J_{10} - J_{20} + (1 - \Delta)J_2(\mathbf{k}) + 2DC_1] - \omega_{1z}}{-(1 - \Delta)J_1(\mathbf{k})} & \frac{[J_{10} - J_{20} + (1 - \Delta)J_2(\mathbf{k}) + 2DC_2] + \omega_{2z}}{-(1 - \Delta)J_1(\mathbf{k})} \end{pmatrix}, \tag{11}$$

$$\mathbf{U}^{-1} = -\frac{(1 - \Delta)J_1(\mathbf{k})}{2\omega_{0z}}\begin{pmatrix} \frac{[J_{10} - J_{20} + (1 - \Delta)J_2(\mathbf{k}) + 2DC_2] + \omega_{2z}}{-(1 - \Delta)J_1(\mathbf{k})} & -1 \\ \frac{[J_{10} - J_{20} + (1 - \Delta)J_2(\mathbf{k}) + 2DC_1] - \omega_{1z}}{(1 - \Delta)J_1(\mathbf{k})} & 1 \end{pmatrix}, \tag{12}$$

where

$$\omega_{\mu z} = \frac{\omega_\mu}{\langle S_\mu^z\rangle} = \sqrt{[J_{10} - J_{20} + (1 - \Delta)J_2(\mathbf{k}) + 2DC_\mu]^2 - [(1 - \Delta)J_1(\mathbf{k})]^2},$$
$$(\mu = 1, 2). \tag{13}$$

Note that we use $\langle S_\mu^z\rangle(\mu = 1, 2)$ to denote the magnetization of the sublattice 1 and 2, and S to denote spin quantum number, and in the present paper S=1. For the frustrated AFM lattice, the exchanges parameter J_1 and J_2 are positive, and when the external field is absent, $\langle S_1^z\rangle = -\langle S_2^z\rangle = \langle S^z\rangle$.

The internal energy $E(T)$ is defined as the thermo-statistical average of the Hamiltonian Eq. (1) per site, $E(T)$= $\langle H\rangle$ /N. The internal energy with considering the spin magnetic correlation effect is expressed in the following:

$$E(T) = \frac{J_{10}}{2}\langle S_1^z\rangle\langle S_2^z\rangle + \frac{J_{20}}{4}(\langle S_1^z\rangle^2 + \langle S_2^z\rangle^2) - \frac{1}{2}D(\langle (S_1^z)^2\rangle + \langle (S_2^z)^2\rangle)$$
$$+ \frac{1}{2}(\Xi_{12}\langle S_2^z\rangle + \Xi_{21}\langle S_1^z\rangle + \Xi_{11}\langle S_1^z\rangle + \Xi_{22}\langle S_2^z\rangle), \tag{14}$$

where

$$\Xi_{\mu\nu} = \begin{cases} \frac{2}{N}\sum_{\mathbf{k}}\sum_{\tau=1}^{2}\frac{U_{\mu\tau}U_{\tau\nu}^{-1}(1 - \Delta)J_2(\mathbf{k})}{e^{\beta\omega_\tau} - 1}, (\mu = \nu); \\ \frac{2}{N}\sum_{\mathbf{k}}\sum_{\tau=1}^{2}\frac{U_{\mu\tau}U_{\tau\nu}^{-1}(1 - \Delta)J_1(\mathbf{k})}{e^{\beta\omega_\tau} - 1}, (\mu \neq \nu). \end{cases} \tag{15}$$

The free energy is evaluated [75] numerically by means of the internal energy $E(T)$ via

$$F(T) = E(0) - T\int_0^T \frac{E(T') - E(0)}{T'^2}dT', \tag{16}$$

where $E(0)$ is the internal energy at T=0. Please note that at T=0, $F(0)$ = $E(0)$.

Eqs. (4–16) are the transcendental equations of sublattice magnetization, internal energy and free energy. From these equations, they can be calculated as a function of temperature, spin anisotropy strength, single-ion anisotropy strength, and frustration strength.

Finally, the expression of Néel temperature is the following:

$$T_N = \frac{S(S + 1)}{3}\frac{1}{\frac{2}{N}\sum_{\mathbf{k}}\left\{\frac{[J_{10} - J_{20} + (1 - \Delta)J_2(\mathbf{k}) + 2DC_1]}{[J_{10} - J_{20} + (1 - \Delta)J_2(\mathbf{k}) + 2DC_1]^2 - [(1 - \Delta)J_1(\mathbf{k})]^2}\right\}}. \tag{17}$$

3. Results and discussions

3.1. Sublattice magnetization and Néel temperature

First of all, the sublattice magnetization is calculated numerically as a function of temperature, frustration strength, spin anisotropy strength, and single-ion anisotropy strength. Fig. 1(a), (b) and (c) plots the normalized temperature T/T_N dependence of the sublattice magnetization $\langle S^z\rangle$ for several spin anisotropy strength Δ values at frustration strength J_2/J_1=0, 0.3, and 0.6, respectively, where the single-ion anisotropy strength D is absent. From Fig. 1(a), (b) and (c), at zero temperature, when Δ‡1, sublattice magnetization $\langle S^z\rangle$ is less than 1, and is dependent on spin anisotropy strength Δ under fixed J_2/J_1. For the case of Δ=1, sublattice magnetization $\langle S^z\rangle$ reaches saturation value 1 for different J_2/J_1 values. This is because even at zero temperature, for the Heisenberg antiferromagnetic systems, the neighboring spins are not rigorously anti-parallel to each other, and there is the spin transverse correlation effect, which is sensitive to the spin anisotropy strength. The larger the spin anisotropy strength Δ, the weaker the spin transverse correlation effect, especially the classical limit Δ=1, the 3D Ising J_1-J_2 model is realized, and transverse spin quantum fluctuations disappear completely, so the $\langle S^z(0)\rangle$ value becomes fully saturated, $\langle S^z(0)\rangle = 1$. The sublattice magnetization $\langle S^z\rangle$ decreases with temperature rising. The temperature at which $\langle S^z\rangle$ becomes zero is the Néel temperature, denoted as T_N. In the following paragraphs, to describe the dependence of the curves on the anisotropy strength Δ and D values, we concentrate our attention to two physical quantities: the sublattice magnetization $\langle S^z\rangle$ at 0 K, and Néel temperature T_N. The former hereafter denoted as $\langle S^z(0)\rangle$, and the latter will be discussed in Fig. 5. Fig. 1 shows that $\langle S^z(0)\rangle$ decreases with Δ increasing. This indicates that transverse spin quantum fluctuation is depressed by spin anisotropy strength Δ. At finite temperature, both quantum and thermodynamic fluctuations appear and become stronger, and they cannot be distinguished. With the increase of normalized temperature T/T_N, the larger the spin anisotropy strength Δ, the slower the sublattice magnetization $\langle S^z\rangle$ drops.

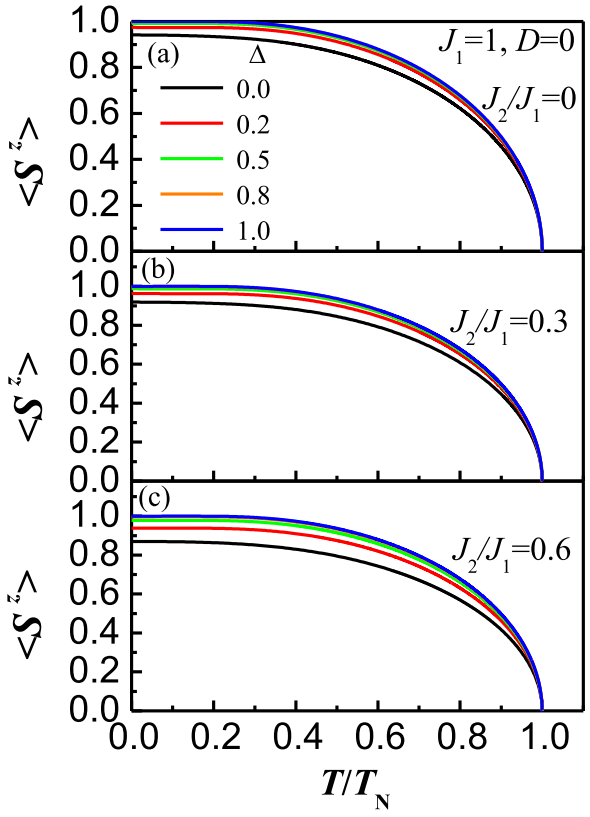

Fig. 1. Sublattice magnetization $\langle S^z \rangle$ as a function of the normalized temperature T/T_N for five values of the spin anisotropies Δ at three frustration strength values: (a) J_2/J_1=0; (b) J_2/J_1=0.3; (c) J_2/J_1=0.6. J_1=1, D=0.

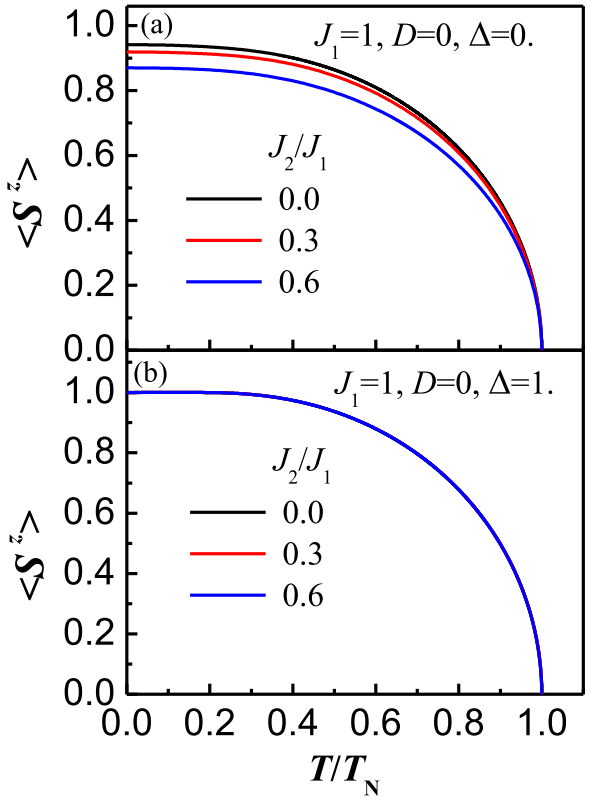

Fig. 2. Sublattice magnetization $\langle S^z \rangle$ as a function of the normalized temperature T/T_N for three values of the frustration strength J_2/J_1 at two spin anisotropies values: (a) Δ=0 (isotropic Heisenberg limit); (b) Δ=1 (Ising limit). J_1=1, D=0.

As mentioned above, When the single-ion anisotropy D is absent, the Hamiltonian Eq. (1) describes the isotropic Heisenberg J_1-J_2 model for Δ=0, and the Ising J_1-J_2 model for Δ=1. In the below, we will compare the magnetization curves ($\langle S^z \rangle$ vs. T/T_N curve) of these two limit cases. Then in Fig. 2(a) and (b) we plot the curves of sublattice magnetization $\langle S^z \rangle$ versus normalized temperature T/T_N for three J_2/J_1 values at two spin anisotropy strength Δ=0 and 1, respectively, and where the single-ion anisotropy D is absent. From Fig. 2(a) and (b), at zero temperature, for the case of isotropic Heisenberg limit (Δ=0), sublattice magnetization $\langle S^z(0) \rangle$ is less than 1, and is dependent on frustration strength J_2/J_1. As J_2/J_1 increases from zero, $\langle S^z(0) \rangle$ decreases. With vanishing nnn interaction J_2=0, the ground state is known to be ordinary antiferromagnets, and there is no competition to cause frustration. As J_2/J_1 increases from zero, the competition between J_2 and J_1 emerges and becomes stronger. This results in the drop of the ground state magnetization $\langle S^z(0) \rangle$. The results are similar for $0 < \Delta < 1$, here the curves have not been drawn. For the case of Ising limit (Δ=1), sublattice magnetization $\langle S^z(0) \rangle$ is equal to 1, which is independent of frustration strength J_2/J_1. Furthermore, from Fig. 2(a) and (b), the larger the spin anisotropy strength Δ, the smaller influence of J_2/J_1 on the $\langle S^z \rangle/S$ vs. T/T_N curve. That is to say, an increase of the spin anisotropy strength reduces the difference of the $\langle S^z \rangle/S$ vs. T/T_N curves at different J_2/J_1 cases. Especially in the case of the classical limit Δ=1, i.e., Ising model, all $\langle S^z \rangle$ vs. T/T_N curves are the same for different J_2/J_1 values. In other words, the frustration strength J_2/J_1 can be used to tune the quantum fluctuations, but it does not play a role in the thermodynamic fluctuations. This result seems indicates that there is a difference between the quantum fluctuations and thermodynamic fluctuations at nonzero temperature, even if they are unable to be distinguished. As a matter of fact, in a quantum magnetic system, there exist both the thermodynamic and quantum fluctuations at finite temperature. The former, from Fig. 2(b), is believed isotropic for different J_2/J_1 values, while the latter, from both Fig. 2(a) and (b), seems to be anisotropic. Let us now return to the Fig. 1, the larger the frustration strength J_2/J_1, the greater influence of Δ on the $\langle S^z \rangle$ vs. T/T_N curve. That is to say, an increase of the J_2/J_1 value enhances the difference of the $\langle S^z \rangle/S$ vs. T/T_N curves at different spin anisotropy strength Δ values. This is the result of the competition between spin anisotropy strength and frustration strength to adjust the quantum fluctuations.

Fig. 3(a), (b) and (c) shows the influence of single-ion anisotropy strength D to the curves of $\langle S^z \rangle/S$ versus T/T_N for J_2/J_1=0, 0.3, and 0.6, respectively, where the spin anisotropy strength Δ is absent. QMC simulation revealed that when the single-ion anisotropy strength D was not too strong, the result calculated by ACs decoupling was better, and closer to those by QMC simulation [75]. Therefore, in the calculation, we take several relatively small D values compared with the J_1=1. Fig. 3 shows that the magnetization $\langle S^z \rangle$ versus T/T_N curve slightly lowers with single-ion anisotropy strength D rising under fixed J_2/J_1 value. At zero temperature, the magnetization $\langle S^z(0) \rangle$ is dependent on single-ion anisotropy strength D under fixed J_2/J_1. The numerical result shows that the magnetization $\langle S^z(0) \rangle$ increases with D rising, as mentioned in the above, the larger the single-ion anisotropy strength, the weaker the spin transverse correlation effect. In one word, this indicates that quantum fluctuations are depressed by single-ion anisotropy strength D.

Fig. 4(a) and (b) plots curves of $\langle S^z(0) \rangle$ versus Δ (D=0) and D (Δ=0) at three J_2/J_1 values, respectively. The curve behaves as follows: under fixed Δ (or D), $\langle S^z(0) \rangle$ decreases with J_2/J_1 rising; under fixed J_2/J_1, $\langle S^z(0) \rangle$ increases with Δ (or D) rising. In addition, for the case of Δ=1, i.e., Ising limit, all sublattice magnetization $\langle S^z(0) \rangle$ are equal to 1 (fully saturated), and independent of frustration strength J_2/J_1. At zero temperature, the thermodynamic fluctuation vanishes but quantum fluctuation still exists in a Heisenberg antiferromagnetic systems. As J_2/J_1 increases from zero, the competition between J_1 and J_2 lowers the $\langle S^z(0) \rangle$ value under fixed Δ (or D). A smaller $\langle S^z(0) \rangle$ value

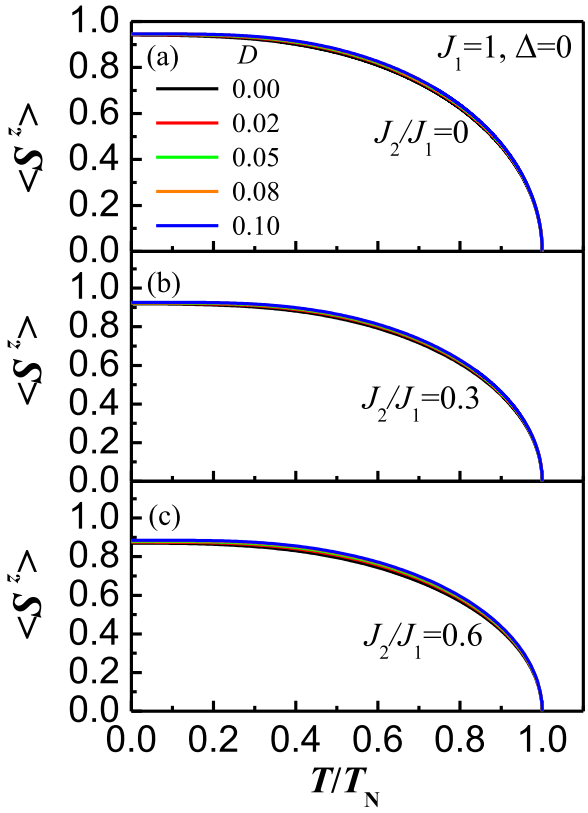

Fig. 3. Sublattice magnetization $\langle S^z \rangle$ as a function of the normalized temperature T/T_N for five values of the single-ion anisotropies D at three frustration strength values: (a) J_2/J_1=0; (b) J_2/J_1=0.3; (c) J_2/J_1=0.6. J_1=1, Δ=0.

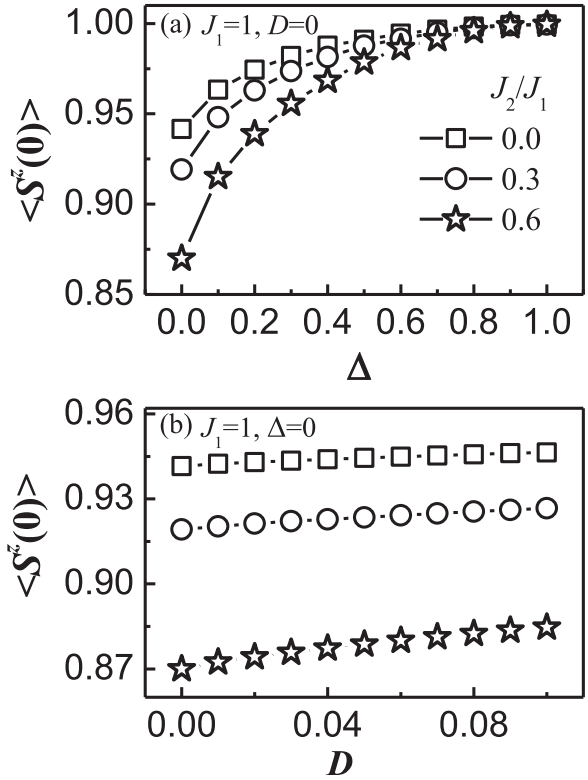

Fig. 4. The ground-state sublattice magnetization $\langle S^z(0) \rangle$ versus (a) spin anisotropy Δ (J_1=1, D=0), and (b) single-ion anisotropy D (J_1=1, Δ=0) for three J_2/J_1 values, respectively. The lines are guides to the eyes.

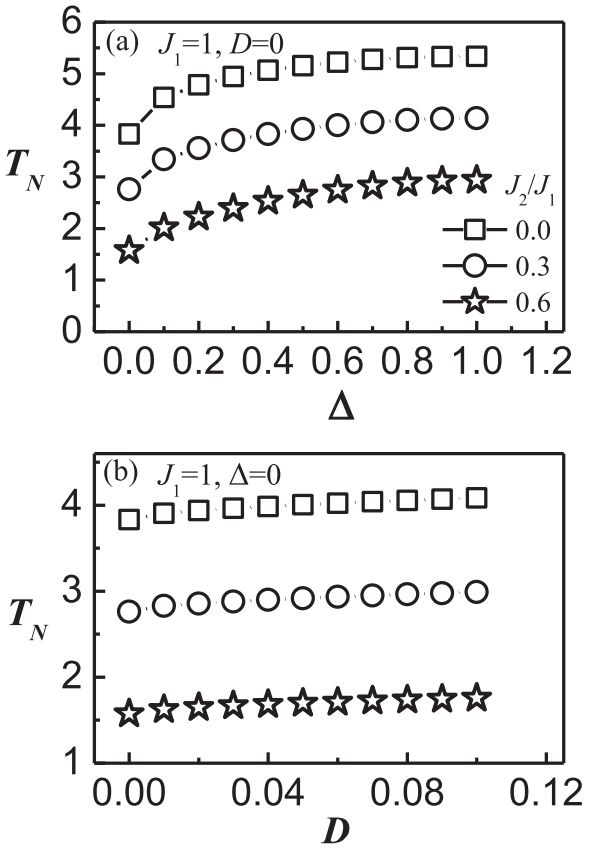

Fig. 5. Néel temperature T_N versus (a) spin anisotropy Δ (J_1=1, D=0), and (b) single-ion anisotropy D (J_1=1, Δ=0) for three J_2/J_1 values, respectively. The lines are guides to the eyes.

represents a stronger quantum fluctuation. In this sense, quantum fluctuation is depressed by spin anisotropy strength and single-ion anisotropy strength, by contrast, is strengthened by frustration strength. Therefore, it is possible to tune the quantum fluctuations by the competition of anisotropy strength and frustration strength to change the ground state properties of magmetic materials.

To illustrate the dependence of Néel temperature on spin anisotropy strength and single-ion anisotropy strength, we plot in Fig. 5(a) and (b) T_N versus Δ (D=0) and D (Δ=0) at three J_2/J_1 values, respectively. From Fig. 5, T_N increases with Δ (or D) rising under fixed J_2/J_1, and decreases with J_2/J_1 rising under fixed Δ (or D). Figs. 4(a) and 5(a) show that frustration strength J_2/J_1does not change the magnetization $\langle S^z(0) \rangle$but can change the Néel temperature T_N for Ising system (Δ=1). Whether it is Heisenberg J_1-J_2 model or Ising J_1-J_2 model, as J_2/J_1 increases from zero, the competition between J_1 and J_2 becomes stronger and it makes T_N lower.

3.2. Internal energy and free energy

Now, let us devote our attention to the internal energy and free energy for Néel phase. The internal energy is mainly composed of the magnetic correlation energy (MCE) and single-ion anisotropy energy. Compared with the former, the latter is relatively small. MCE is the sum of the transverse correlation energy (TCE) and longitudinal correlation energy (LCE), the former is easily calculated precisely by means of the well-known spectral theorem, the latter, however, is not easy to evaluate precisely, and some approximations are inevitable. Here we use the RPA approximation as expressed in Ref. [60], and which neglects the short range correlation effect, especially in the vicinity of the Néel temperature. The free energy can be evaluated numerically by means of the internal energy $E(T)$ via Eq. (16).

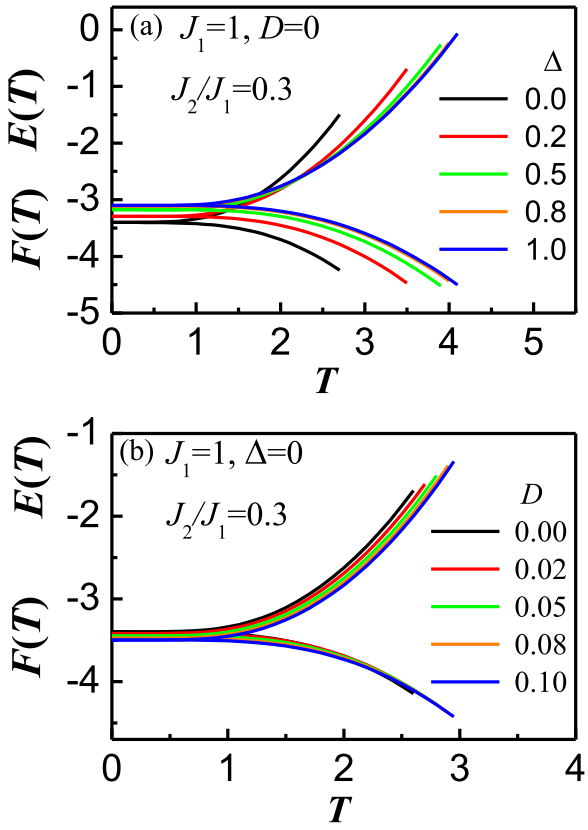

Fig. 6. The internal energies (ascending curves) and free energies (descending curves) versus temperature for (a) several spin anisotropy Δ (J_1=1, D=0), and (b) several single-ion anisotropy D (J_1=1, Δ=0) as J_2/J_1=0.3.

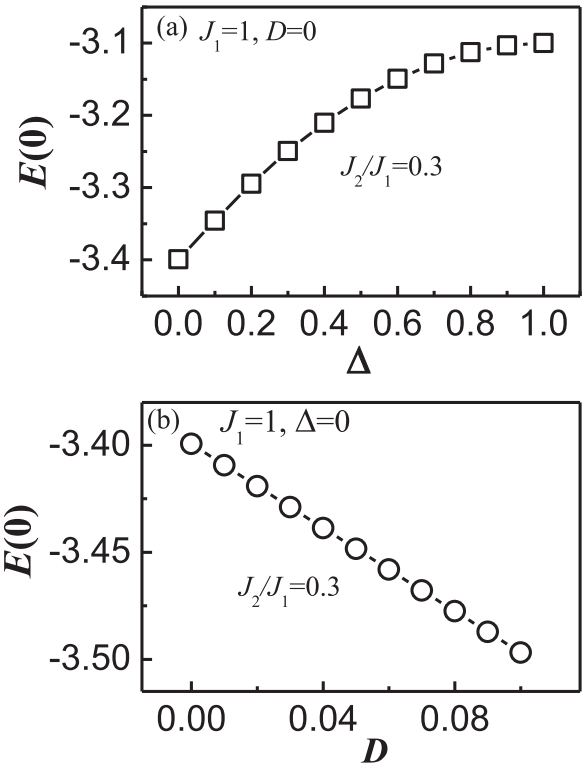

Fig. 7. The ground-state energy $E(0)$ versus (a) spin anisotropy Δ (J_1=1, D=0), and (b) single-ion anisotropy D (J_1=1, Δ=0) as J_2/J_1=0.3, respectively. The lines are guides to the eyes.

Fig. 6(a) plots the temperature dependence of the internal energies and free energies for several spin anisotropy strength Δ values at J_2/J_1=0.3, where the single-ion anisotropy D is absent. The internal energy $E(T)$ increases with temperature monotonically as it should be. While the corresponding free energies decreases monotonically with temperature. It is seen that the values of internal energy and the corresponding free energy are the same at zero temperature. At zero temperature, under fixed J_2/J_1 =0.3, the larger the spin anisotropy strength Δ is, the higher the internal energy is, and the free energy as well. At finite temperature, with the increase of temperature, the smaller the spin anisotropy strength, the faster the internal energy rises, so that the internal energy curves at different spin anisotropy strength Δ cross each other at some temperature values. Especially when the temperature is greater than a certain value, the internal energy curve drops with the increase of spin anisotropy strength. Unlike internal energy, free energy curve does not cross each other, the larger the spin anisotropy strength, the higher the free energy curve.

Fig. 6(b) plots the temperature dependence of the internal energies and free energies for several single-ion anisotropy D values at J_2/J_1=0.3, where the spin anisotropy strength Δ is absent. At zero temperature, the larger the single-ion anisotropy strength D is, the lower the internal energy is, and the free energy as well. At finite temperature, Fig. 3(b) shows that the internal energy decreases with D rising under fixed temperature. With the increase of temperature, the smaller the single-ion anisotropy strength D, the faster the free energy falls, and the free energy decreases more rapidly at a lower temperature than at a higher temperature, so that the free energy curves at different single-ion anisotropy strength D cross each other at some temperature values.

From Fig. 6(a) and (b), we see that the effects of Δ and D on energies are different. We mainly focus on the case of zero temperature. In Fig. 7(a) and (b) we plot the ground-state energy $E(0)$ as a function of the Δ (D=0) and D (Δ=0) at J_2/J_1=0.3, respectively. Fig. 7(a) and (b) shows that the ground-state energy increases with the spin anisotropy strength Δ rising, and decreases linearly with the single-ion anisotropy strength D increasing, respectively. This seems indicates that the quantum phase transition may be more likely to occur for the larger Δ and the smaller D value at a suitable parameter J_2/J_1. The concerned quantum phase transition remains to be further studied in the near further.

3.3. Comparison of the effect of the Δ and D on the thermodynamic quantities

As mentioned in the introduction, anisotropies, either spin anisotropy or single-ion anisotropy, are likely to be present in real magnetic materials. They both suppress the quantum fluctuations, but they originate from very different physical mechanisms. In the last part, we compare the effect of the spin anisotropy strength and single-ion anisotropy strength on the sublattice magnetization and internal energy curves. Fig. 8(a), (b), (c) and (d) plots the temperature T dependence of the sublattice magnetization $\langle S^z\rangle$ for four sets of parameter Δ and D values at frustration strength J_2/J_1=0.3, respectively. Correspondingly, Fig. 9(a), (b), (c) and (d) plots the temperature T dependence of the corresponding internal energies $E(T)$ for four sets of parameter Δ and D values at frustration strength J_2/J_1=0.3, respectively. We see from Fig. 8(a) and Fig. 9(a) that the behaviors of the sublattice magnetization and internal energy in the cases Δ=0.001, D=0.003 and Δ=0.003, D=0.001 are almost identical, respectively. We also see from Figs. 8(b) and 9(b) that the behaviors of the sublattice magnetization and internal energy in the cases Δ=0.01, D=0.03 and Δ=0.03, D=0.01 are very similar, respectively. The numerical results indicate that the spin anisotropy and single-ion anisotropy are almost equivalent for a small set of parameter values. However, Figs. 8(c) and 9(c) shows that the differences of the sublattice magnetization and internal energy curves increase for a larger set of

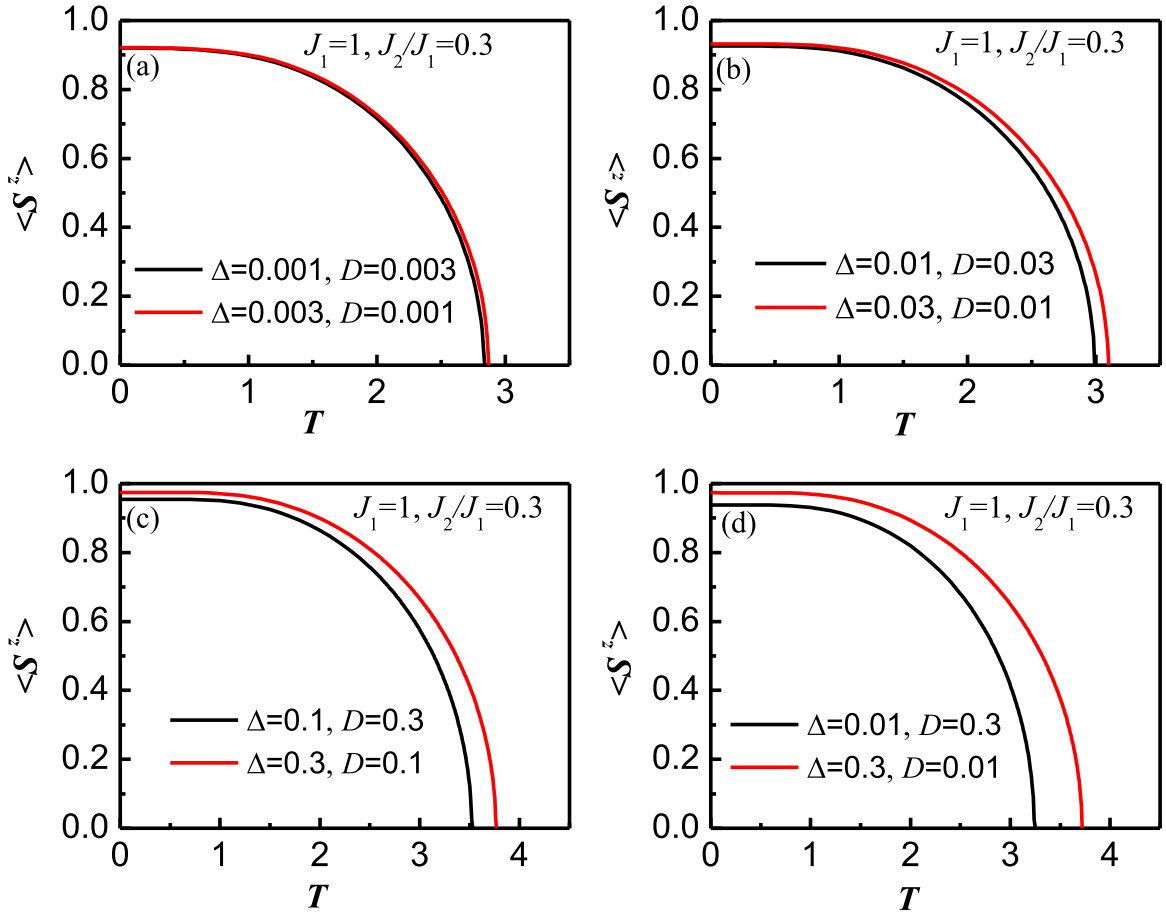

Fig. 8. Sublattice magnetization $\langle S^z \rangle$ versus temperature T for J_1=1 and J_2/J_1=0.3 at four sets of parameter values: (a) Δ=0.001 (0.003), D=0.003 (0.001); (b) Δ=0.01 (0.03), D=0.03 (0.01); (c) Δ=0.1 (0.3), D=0.3 (0.1); (d) Δ=0.01 (0.3), D=0.3 (0.01).

parameters Δ=0.1, D=0.3 and Δ=0.3, D=0.1, respectively. In this case, the spin anisotropy and single-ion anisotropy are not equivalent. Which anisotropy has a larger effect on the thermodynamic quantity? Figs. 8(d) and 9(d) shows that the effect of the spin anisotropy on the thermodynamic quantities is larger than that of the single-ion anisotropy. Therefore, it is possible to propose an experiment based on our results that could decide which kind of anisotropy is acting in a real 3D antiferromagnetic material.

4. Concluding remarks

In this paper, the magnetic and thermodynamic properties of frustrated anisotropic spin-1 Heisenberg antiferromagnet on a bcc lattice for Néel phase are systematically investigated by use of the double-time Green's function method within the RPA and ACs decoupling. The role of spin anisotropy strength, single-ion anisotropy strength, respectively, and both of them on thermodynamic quantities (sublattice magnetization, Néel temperature, internal energy, and free energy) are carefully calculated and analyzed, and the effect of both of the spin anisotropy strength and frustration strength on the $\langle S^z \rangle$ vs. T/T_N curve is also discussed.

The zero-temperature sublattice magnetization and Néel temperature increase with spin anisotropy strength and single-ion anisotropy strength, and decrease with frustration strength. This indicates that quantum fluctuation is depressed by spin anisotropy strength and single-ion anisotropy strength, by contrast, is strengthened by frustration strength. It is possible to tune the quantum fluctuations by the competition of anisotropy strength and frustration strength to change the ground state properties of magmetic materials. The larger the frustration strength J_2/J_1 is, the greater influence of spin anisotropy strength Δ on the $\langle S^z \rangle$ vs. T/T_N curve. The larger the spin anisotropy strength Δ is, the smaller influence of J_2/J_1 on the $\langle S^z \rangle/S$ vs. T/T_N curve. Especially in the case of the classical limit Δ=1, i.e., Ising model, all $\langle S^z \rangle$ vs. T/T_N curves are the same for different J_2/J_1 values. In other words, the frustration strength J_2/J_1can be used to tune the quantum fluctuations, but it does not play a role in the thermodynamic fluctuations. As a matter of fact, in a quantum magnetic system, there exist both the thermodynamic and quantum fluctuations at finite temperature. The former, from Fig. 2(b), is believed isotropic for different J_2/J_1 values, while the latter, from both Fig. 2(a) and (b), seems to be anisotropic.

Although we find that both the spin anisotropy and the single-ion anisotropy suppress the quantum fluctuations, but their respective effects on the thermodynamic quantities, especially the internal energy and free energy, are different at zero temperature and finite temperature. At zero temperature, the internal energy and free energy increase with spin anisotropy strength, and decrease with single-ion anisotropy strength. At finite temperature, when the single-ion anisotropy is absent, with the increase of temperature, the smaller the spin anisotropy strength, the faster the internal energy rises, so that the internal energy curves at different spin anisotropy strength cross each other at some temperature values. Especially when the temperature is greater than a certain value, the internal energy curve drops with the increase of spin anisotropy strength. Unlike internal energy, free energy curve does not cross each other, the larger the spin anisotropy strength, the higher the free energy curve. On the contrary, when the spin anisotropy is absent, the internal energy decreases with single-ion anisotropy strength rising under any fixed temperature. With the increase of temperature, the smaller the single-ion anisotropy strength, the faster the free energy falls, and the free energy decreases more

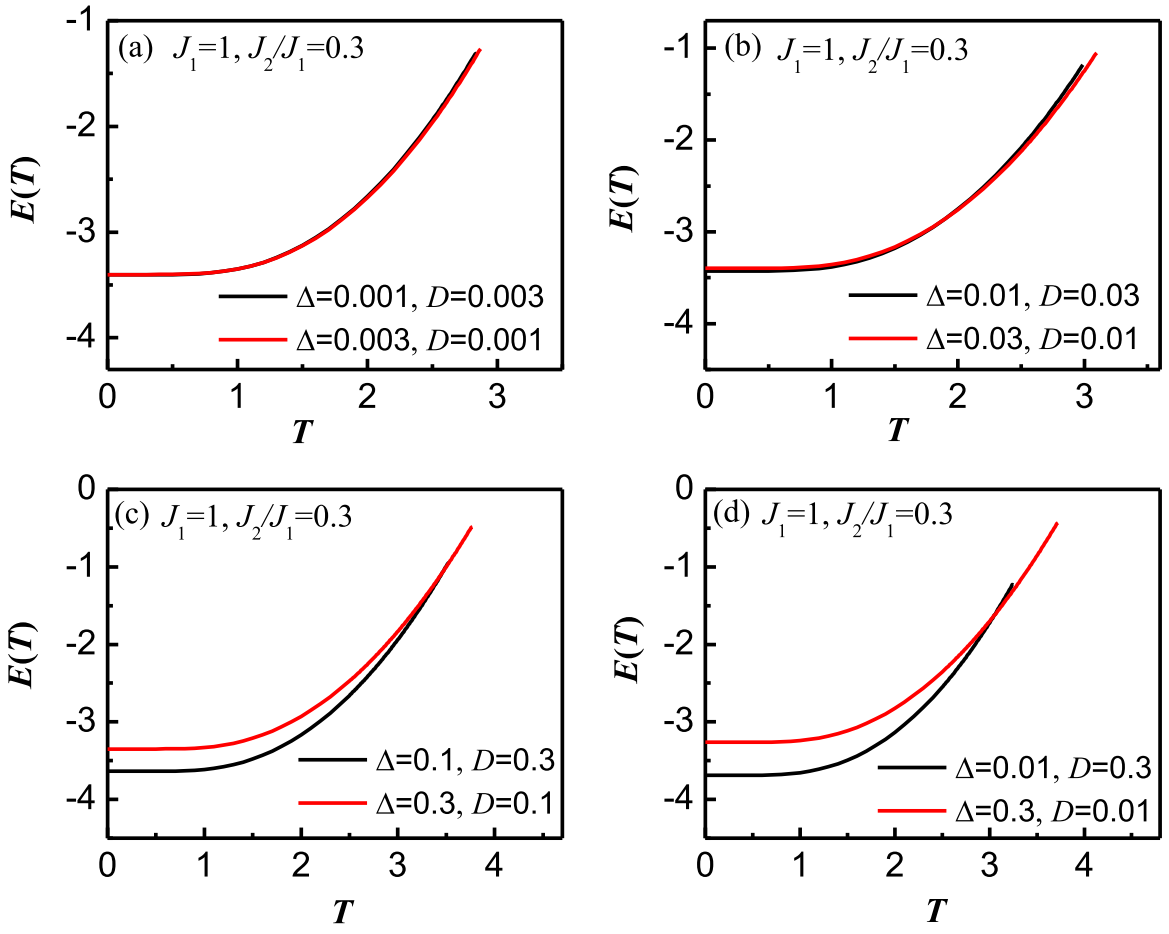

Fig. 9. Internal energy $E(T)$ versus temperature T for J_1=1 and J_2/J_1=0.3 at four sets of parameter values: (a) Δ=0.001 (0.003), D=0.003 (0.001); (b) Δ=0.01 (0.03), D=0.03 (0.01); (c) Δ=0.1 (0.3), D=0.3 (0.1); (d) Δ=0.01 (0.3), D=0.3 (0.01).

rapidly at a lower temperature than at a higher temperature, so that the free energy curves at different single-ion anisotropy strength cross each other at some temperature values.

The numerical results indicate that both of the spin anisotropy and single-ion anisotropy are almost equivalent for a small set of parameter values (Δ and D) and are not equivalent for a larger set of parameter values (Δ and D). Furthermore, when these two kinds of anisotropic coexist, the effect of the spin anisotropy on the thermodynamic quantities is larger than that of the single-ion anisotropy. Therefore, it is possible to propose an experiment based on our results that could decide which kind of anisotropy is acting in a real 3D antiferromagnetic material.

Acknowledgements

The author would like to thank Prof. Qiang Gu for illuminating discussions. This work was supported by the National Natural Science Foundation of China (Grant No. 11574028), the Langfang City Key Technology Research and Development Program of China (Grant No. 2016011036), and the Higher Educational Science and Technology Research Project of Hebei Province of China (Grant No. ZC2016075).

References

[1] Introduction to frustrated magnetism: materials, experiments, theory, in: C. Lacroix, P. Mendels, F. Mila (Eds.), , Series in Solid-State Sciences 164, Springer, Berlin, 2011.
[2] S. Sachdev, Quantum Phase Transitions, 1st ed, Cambridge University Press, Cambridge, 2001.
[3] H.T. Diep, Frustrated Spin Systems, 1st ed, World Scientific Publishing Co. Pte. Ltd, Singapore, 2004.
[4] E. Dagotto, A. Moreo, Phys. Rev. Lett. 63 (1989) 2148.
[5] E. Manousakis, Rev. Mod. Phys. 63 (1991) 1.
[6] H. Rosner, R.R.P. Singh, W.H. Zheng, J. Oitmaa, W.E. Pickett, Phys. Rev. B 67 (2003) 014416.
[7] J. Sirker, Zheng Weihong, O.P. Sushkov, J. Oitmaa, Phys. Rev. B 73 (2006) 184420.
[8] Y. Kamihara, T. Watanabe, M. Hirano, H. Hosono, J. Am. Chem. Soc. 130 (2008) 3296.
[9] H.H. Wen, G. Mu, L. Fang, H. Yang, X. Zhu, Europhys. Lett. 82 (2008) 17009.
[10] H. Takahashi, K. Igawa, K. Arii, Y. Kamihara, M. Hirano, H. Hosono, Nat. (Lond.) 453 (2008) 376.
[11] C.D.L. Cruz, Q. Huang, J.W. Lynn, J. Li, W. Ratcliff, J.L. Zarestky, H.A. Mook, G.F. Chen, J.L. Luo, N.L. Wang, P. Dai, Nature 453 (2008) 899 (London).
[12] X.H. Chen, T. Wu, G. Wu, R.H. Liu, H. Chen, D.F. Fang, Nature 453 (2008) 761 (London).
[13] G.F. Chen, Z. Li, D. Wu, G. Li, W.Z. Hu, J. Dong, P. Zheng, J.L. Luo, N.L. Wang, Phys. Rev. Lett. 100 (2008) 247002.
[14] Z.A. Ren, J. Yang, W. Lu, W. Yi, X.L. Shen, Z.C. Li, G.C. Che, X.L. Dong, L.L. Sun, F. Zhong, Z.X. Zhao, Europhys. Lett. 82 (2008) 57002.
[15] M. Rotter, M. Tegel, D. Johrendt, Phys. Rev. Lett. 101 (2008) 107006.
[16] H.J. Schulz, T.A.L. Ziman, Europhys. Lett. 18 (1992) 355.
[17] J. Richter, Phys. Rev. B 47 (1993) 5794.
[18] J. Richter, N.B. Ivanov, K. Retzlaff, Europhys. Lett. 25 (1994) 545.
[19] R.R.P. Singh, Zheng Weihong, C.J. Hamer, J. Oitmaa, Phys. Rev. B 60 (1999) 7278.
[20] L. Capriotti, S. Sorella, Phys. Rev. Lett. 84 (2000) 3173.
[21] O.P. Sushkov, J. Oitmaa, Zheng Weihong, Phys. Rev. B 63 (2001) 104420.
[22] R.R.P. Singh, W. Zheng, J. Oitmaa, O.P. Sushkov, C.J. Hamer, Phys. Rev. Lett. 91 (2003) 017201.
[23] F. Krüger, S. Scheidl, Europhys. Lett. 74 (2006) 896.
[24] R. Darradi, O. Derzhko, R. Zinke, J. Schulenburg, S.E. Krüger, J. Richter, Phys. Rev. B 78 (2008) 214415.
[25] J. Richter, J. Schulenburg, Eur. Phys. J. B 73 (2010) 117.
[26] Shou-Shu Gong, Wei Zhu, D.N. Sheng, Olexei I. Motrunich, Matthew P.A. Fisher, Phys. Rev. Lett. 113 (2014) 027201.
[27] Johannes Richter, Ronald Zinke, Damian J.J. Farnell, Eur. Phys. J. B 88 (2015) 2.
[28] T.P. Cysne, M.B. Silva Neto, Europhys. Lett. 112 (2015) 47002.
[29] Yong-Zhi Ren, Ning-Hua Tong, Xin-Cheng Xie, , J. Phys.: Condens. Matter 26 (2014) 115601.
[30] Carlene Farias, Christopher Thomas, Catherine Pépin, Alvaro Ferraz, Claudine Lacroix, S.ébastien Burdin, Phys. Rev. B 94 (2016) 134420.

[31] B. Canals, C. Lacroix, Phys. Rev. Lett. 80 (1998) 2933.
[32] Akihisa Koga, Norio Kawakami, Phys. Rev. B 63 (2001) 144432.
[33] J. Villain, J. Phys. Chem. Solids 11 (1959) 303.
[34] H.T. Diep, Phys. Rev. B 39 (1989) 397.
[35] H.T. Diep, Phys. Rev. B 40 (1989) 741.
[36] E. Rastelli, S. Sedazzari, A. Tassi, J. Phys.: Condens. Matter 1 (1989) 4735.
[37] E. Rastelli, S. Sedazzari, A. Tassi, J. Phys.: Condens. Matter 2 (1990) 8935.
[38] R. Quartu, H.T. Diep, J. Magn. Magn. Mater. 182 (1998) 38.
[39] D. Loison, Physica A 275 (2000) 207.
[40] A.O. Sorokin, A.V. Syromyatnikov, J. Exp. Theor. Phys. 113 (2011) 673.
[41] C. Pépin, M.R. Norman, S. Burdin, A. Ferraz, Phys. Rev. Lett. 106 (2011) 106601.
[42] Christopher Thomas, S.ébastien Burdin, Catherine Pépin, Alvaro Ferraz, Phys. Rev. B 87 (2013) 014422.
[43] T. Roscilde, A. Feiguin, A.L. Chernyshev, S. Liu, S. Haas, Phys. Rev. Lett. 93 (2004) 017203.
[44] J.R. Viana, J.R. de Sousa, Phys. Rev. B 75 (2007) 052403.
[45] R.F. Bishop, P.H.Y. Li, R. Darradi, J. Schulenburg, J. Richter, Phys. Rev. B 78 (2008) 054412.
[46] R. Darradi, J. Richter, J. Schulenburg, R.F. Bishop, P.H.Y. Li, J. Phys.: Conf. Ser. 145 (2009) 012049.
[47] R.F. Bishop, P.H.Y. Li, D.J.J. Farnell, C.E. Campbell, Phys. Rev. B 79 (2009) 174405.
[48] R.F. Bishop, P.H.Y. Li, D.J.J. Farnell, C.E. Campbell, Phys. Rev. B 82 (2010) 024416.
[49] A.S.T. Pires, Solid State Commun. 193 (2014) 56.
[50] Wang Huai-Yu, Phys. Rev. B 86 (2012) 144411.
[51] Ai-Yuan Hu, Huai-Yu Wang, Phys. Rev. E 93 (2016) 012108.
[52] Ai-Yuan Hu, Huai-Yu Wang, Phys. Rev. E 94 (2016) 012142.
[53] J.S. Smart, Effective Field Theories of Magnetism, Saunders, Philadelphia, 1966.
[54] R. Schmidt, J. Schulenburg, J. Richter, Phys. Rev. B 66 (2002) 224406.
[55] J. Oitmaa, W. Zhang, Phys. Rev. B 69 (2004) 064416.
[56] K. Majumdar, T. Datta, J. Phys.: Condens. Matter 21 (2009) 406004.
[57] D.J.J. Farnell, O. Götze, J. Richter, Phys. Rev. B 93 (2016) 235123.
[58] M.R. Pantić, D.V. Kapor, S.M. Radošević, P.M. Mali, Solid State Commun. 182 (2014) 55.
[59] Johannes Richter, Patrick Müller, Andre Lohmann, Heinz-J.ürgen Schmidt, Phys. Procedia 75 (2015) 813–820.
[60] Bin-Zhou Mi, Solid State Commun. 239 (2016) 20–26.
[61] Michael Holt, Oleg P. Sushkov, Daniel Stanek, G.ötz S. Uhrig, Phys. Rev. B 83 (2011) 144528.
[62] Onofre Rojas, C.J. Hamer, J. Oitmaa, J. Phys.: Condens. Matter 23 (2011) 416001.
[63] Zhuo Fan, Quan-lin Jie, Phys. Rev. B 89 (2014) 054418.
[64] Md. Mahfoozul Haque, M.A.H. Ahsan, arXiv 1603 (2016) 02601v2.
[65] Fengjie Ma, Zhong-Yi Lu, Tao Xiang, Phys. Rev. B 78 (2008) 224517.
[66] T. Yildirim, Phys. Rev. Lett. 101 (2008) 057010.
[67] Qimiao Si, Elihu Abrahams, Phys. Rev. Lett. 101 (2008) 076401.
[68] Y. Nishihara, Y. Yamaguchi, T. Kohara, M. Tokumoto, Phys. Rev. B 31 (1985) 5775.
[69] Y. Nishihara, Y. Yamaguchi, M. Tokumoto, K. Takeda, K. Fukamichi, Phys. Rev. B 34 (1986) 3446.
[70] Mari Einaga, Ayako Ohmura, Atsuko Nakayama, Fumihiro Ishikawa, Yuh Yamada, Satoshi Nakano, Phys. Rev. B 83 (2011) 092102.
[71] H. Callen, Phys. Rev. 130 (1963) 890.
[72] N. Majlis, The Quantum Theory of Magnetism, World Scientific, Singapore, 2000.
[73] S. Schwieger, J. Kienert, W. Nolting, Phys. Rev. B 71 (2005) 024428.
[74] M.G. Pini, P. Politi, R.L. Stamps, Phys. Rev. B 72 (2005) 014454.
[75] P. Fröbrich, P.J. Kuntz, Phys. Rep. 432 (2006) 223.
[76] Huai-Yu Wang, Green's Function in Condensed Matter Physics, Alpha Science International Ltd. and Science Press, Beijing, 2012.
[77] Bin-Zhou Mi, Huai-Yu Wang, Yun-Song Zhou, J. Magn. Magn. Mater. 322 (2010) 952.
[78] M.S. Rutonjski, S.M. Radošević, M.R. Pantić, M.V. Pavkov-Hrvojević, D.V. Kapor, M.G. Škrinjar, Solid State Commun. 151 (2011) 518.
[79] S.M. Radošević, M.S. Rutonjski, M.R. Pantić, M.V. Pavkov-Hrvojević, D.V. Kapor, M.G. Škrinjar, Solid State Commun. 151 (2011) 1753.
[80] G. Mert, H.S. Mert, Physica A 391 (2012) 5926.